



UNH-07-01
UCRL-JRNL-231719
UMD-40762-391
JLAB-THY-07-653
NT@UW-07-08

Precise Determination of the $I = 2$ $\pi\pi$ Scattering Length from Mixed-Action Lattice QCD

Silas R. Beane,¹ Thomas C. Luu,² Kostas Orginos,^{3,4} Assumpta Parreño,⁵ Martin J. Savage,⁶ Aaron Torok,¹ and André Walker-Loud⁷

(NPLQCD Collaboration)

¹*Department of Physics, University of New Hampshire, Durham, NH 03824-3568.*

²*N Division, Lawrence Livermore National Laboratory, Livermore, CA 94551.*

³*Department of Physics, College of William and Mary, Williamsburg, VA 23187-8795.*

⁴*Jefferson Laboratory, 12000 Jefferson Avenue, Newport News, VA 23606.*

⁵*Departament d'Estructura i Constituents de la*

Matèria and Institut de Ciències del Cosmos,

Universitat de Barcelona, E-08028 Barcelona, Spain.

⁶*Department of Physics, University of Washington, Seattle, WA 98195-1560.*

⁷*Department of Physics, University of Maryland, College Park, MD 20742-4111.*

Abstract

The $I = 2$ $\pi\pi$ scattering length is calculated in fully-dynamical lattice QCD with domain-wall valence quarks on the asqtad-improved coarse MILC configurations (with fourth-rooted staggered sea quarks) at four light-quark masses. Two- and three-flavor mixed-action chiral perturbation theory at next-to-leading order is used to perform the chiral and continuum extrapolations. At the physical charged pion mass, we find $m_\pi a_{\pi\pi}^{I=2} = -0.04330 \pm 0.00042$, where the error bar combines the statistical and systematic uncertainties in quadrature.

I. INTRODUCTION

Pion-pion ($\pi\pi$) scattering at low energies is the simplest and best-understood hadron-hadron scattering process. Its simplicity and tractability follow from the fact that the pions are identified as the pseudo-Goldstone bosons associated with the spontaneous breaking of the approximate chiral symmetry of Quantum Chromodynamics (QCD). For this reason, the low-momentum interactions of pions are strongly constrained by the approximate chiral symmetries, more so than other hadrons. The scattering lengths for $\pi\pi$ scattering in the s-wave are uniquely predicted at leading order (LO) in chiral perturbation theory (χ -PT) [1]:

$$m_\pi a_{\pi\pi}^{I=0} = 0.1588 \quad ; \quad m_\pi a_{\pi\pi}^{I=2} = -0.04537 \quad , \quad (1)$$

at the charged pion mass. Subleading orders in the chiral expansion of the $\pi\pi$ amplitude give rise to perturbatively-small deviations from the tree level, and contain both calculable non-analytic contributions and analytic terms with new coefficients that are not determined by chiral symmetry alone [2, 3, 4]. In order to have predictive power at subleading orders, these coefficients must be obtained from experiment or computed with lattice QCD.

Recent experimental efforts have been made to compute the s-wave $\pi\pi$ scattering lengths, $a_{\pi\pi}^{I=0}$ ($I = 0$) and $a_{\pi\pi}^{I=2}$ ($I = 2$): E865 [5, 6] (K_{e4} decays), CERN DIRAC [7] (pionium lifetime) and CERN NA48/2 [8] ($K^\pm \rightarrow \pi^\pm \pi^0 \pi^0$). Unfortunately, these experiments do not provide stringent constraints on $a_{\pi\pi}^{I=2}$. However, a theoretical determination of s-wave $\pi\pi$ scattering lengths which makes use of experimental data has reached a remarkable level of precision [9, 10]:

$$m_\pi a_{\pi\pi}^{I=0} = 0.220 \pm 0.005 \quad ; \quad m_\pi a_{\pi\pi}^{I=2} = -0.0444 \pm 0.0010 \quad . \quad (2)$$

These values result from the Roy equations [11, 12, 13], which use dispersion theory to relate scattering data at high energies to the scattering amplitude near threshold. In a striking recent result, this technology has allowed a model-independent determination of the mass and width of the resonance with vacuum quantum numbers (the σ meson) that appears in the $\pi\pi$ scattering amplitude [14]. Several low-energy constants of one-loop χ -PT are critical inputs to the Roy equation analysis. One can take the values of these low-energy constants computed with lattice QCD by the MILC collaboration [15, 16] as inputs to the Roy equations, and obtain results for the scattering lengths consistent with the analysis of Ref. [9].

A direct lattice QCD determination of threshold $\pi\pi$ scattering is problematic in two respects. First, the occurrence of disconnected diagrams in the $I = 0$ s-wave channel renders a determination of that amplitude very costly in terms of computer time, given the current state of lattice algorithms, and is thus beyond our current capabilities. As a result, lattice QCD efforts have focused on the $I = 2$ channel. The second difficulty is due to the fact that lattice QCD calculations are performed on a Euclidean lattice. The Maiani-Testa theorem demonstrates that S-matrix elements cannot be determined from lattice calculations of n -point Green's functions at infinite volume, except at kinematic thresholds [17]. This difficulty was overcome by Lüscher, who showed that by computing the energy levels of two-particle states in the finite-volume lattice, the $2 \rightarrow 2$ scattering amplitude can be recovered [18, 19, 20, 21, 22]. The energy levels of the two interacting particles are found to deviate from those of two non-interacting particles by an amount that depends on the scattering amplitude and varies inversely with the lattice spatial volume.

The first lattice calculations of $\pi\pi$ scattering were performed in quenched QCD [23, 24, 25, 26, 27, 28, 29, 30, 31, 32, 33, 34, 35, 36, 37, 38, 39, 40, 41, 42], and the first full-QCD calculation of $\pi\pi$ scattering (the scattering length and phase-shift) was carried through by the CP-PACS collaboration, who exploited the finite-volume strategy to study $I = 2$, s-wave scattering with two flavors ($n_f = 2$) of improved Wilson fermions [43], with pion masses in the range $m_\pi \simeq 0.5 - 1.1$ GeV. The first fully-dynamical calculation of the $I = 2$ $\pi\pi$ scattering length with three flavors ($n_f = 2 + 1$) of light quarks was performed by some of the present authors using domain-wall valence quarks on asqtad-improved staggered sea quarks at four pion masses in the range $m_\pi \simeq 0.3 - 0.5$ GeV at a single lattice spacing, $b \sim 0.125$ fm [44]. That work quoted a value of the scattering length extrapolated to the physical point of

$$m_\pi a_{\pi\pi}^{I=2} = -0.0426 \pm 0.0006 \pm 0.0003 \pm 0.0018 \quad , \quad (3)$$

where the first uncertainty is statistical, the second is a systematic due to fitting and the third uncertainty is due to truncation of the chiral expansion.

In this paper we update our fully-dynamical mixed-action calculation of the $I = 2$ $\pi\pi$ scattering length. Two recent developments motivate an update: i) we have vastly increased statistics at the three light-quark masses studied in the original publication; ii) $\pi\pi$ scattering has been computed with Mixed-Action χ -PT (MA χ -PT) at next-to-leading order (NLO) [45, 46] both for two and three flavors of light quarks. Our updated result is:

$$m_\pi a_{\pi\pi}^{I=2} = -0.04330 \pm 0.00042 \quad , \quad (4)$$

where the statistical and systematic uncertainties have been combined in quadrature. This result is consistent with all previous determinations within uncertainties.

This paper is organized as follows. In Section II details of our mixed-action lattice QCD calculation are presented. We refer the reader interested in a more comprehensive treatment and discussion to our earlier papers. Discussion of the relevant correlation functions and an outline of the methodology and fitting procedures can also be found in this section. The results of the lattice calculation and the analysis with two- and three-flavor MA χ -PT are presented in Section III. In Section IV, the various sources of systematic uncertainty are identified and quantified. In Section V we conclude.

II. METHODOLOGY AND DETAILS OF THE LATTICE CALCULATION

The computation in this paper uses the mixed-action lattice QCD scheme developed by LHPC [47, 48]. Domain-wall fermion propagators were generated from a smeared source on $n_f = 2 + 1$ asqtad-improved [49, 50] coarse configurations generated with rooted staggered sea quarks [51]. Hypercubic-smeared (HYP-smeared) [52, 53, 54, 55] gauge links were used in the domain-wall fermion action to improve chiral symmetry (further details about the mixed-action scheme can be found in Refs. [56, 57]). The mixed-action calculations we have performed involved computing the valence-quark propagators using the domain-wall formulation of lattice fermions, on each gauge-field configuration of an ensemble of the coarse MILC lattices that are generated using the staggered formulation of lattice fermions [58, 59, 60, 61, 62] and taking the fourth root of the fermion determinant, i.e. domain-wall valence quarks on a rooted-staggered sea. In the continuum limit the $n_f = 2$ staggered action has an $SU(8)_L \otimes SU(8)_R \otimes U(1)_V$ chiral symmetry due to the four-fold taste degeneracy of each

TABLE I: The parameters of the MILC gauge configurations and domain-wall propagators used in this work. The subscript l denotes light quark (up and down), and s denotes the strange quark. The superscript dwf denotes the bare-quark mass for the domain-wall fermion propagator calculation. The last column is the number of configurations times the number of sources per configuration.

Ensemble	bm_l	bm_s	bm_l^{dwf}	bm_s^{dwf}	$10^3 \times bm_{res}^a$	# of propagators
2064f21b676m007m050	0.007	0.050	0.0081	0.081	1.604 ± 0.038	468×16
2064f21b676m010m050	0.010	0.050	0.0138	0.081	1.552 ± 0.027	658×20
2064f21b679m020m050	0.020	0.050	0.0313	0.081	1.239 ± 0.028	486×24
2064f21b681m030m050	0.030	0.050	0.0478	0.081	0.982 ± 0.030	564×8

^aComputed by the LHP collaboration.

flavor, and each pion has 15 degenerate additional partners. At finite lattice spacing this symmetry is broken and the taste multiplets are no longer degenerate, but have splittings that are $\mathcal{O}(\alpha^2 b^2)$. While there is no proof, there are arguments to suggest that taking the fourth root of the fermion determinant recovers the contribution from a single Dirac fermion ¹. The results of this paper assume that the fourth-root trick recovers the correct continuum limit of QCD.

When determining the mass of the valence quarks there is an ambiguity due to the non-degeneracy of the 16 staggered bosons associated with each pion. One could choose to match to the taste-singlet meson or to any of the mesons that become degenerate in the continuum limit. Given that the effective field theory exists to describe such calculations at finite lattice spacing, the effects of matching can be described, and removed, by effective field theory calculations appropriate to the choice of matching. The quantity $b^2 \Delta_I$ is the mass-difference between a valence meson and the staggered taste-singlet meson when the valence pion is tuned to be exactly degenerate with the lightest staggered pion. On the coarse MILC lattices with $b \sim 0.125$ fm (and $L \sim 2.5$ fm) it is numerically determined (in lattice units) that $b^2 \Delta_I = 0.0769(22)$ [15].

A summary of the lattice parameters and resources used in this work is given in Table I. In order to generate large statistics on the existing MILC configurations, multiple propagators from sources displaced both temporally and spatially on the lattice were computed. The correlators were blocked so that one average correlator per configuration was used in the subsequent Jackknife statistical analysis (that will be described later).

The π correlation function, $C_\pi(t)$, and the $\pi\pi$ correlation function $C_{\pi\pi}(p, t)$ were computed, where the number of time slices between the hadronic sink and the hadronic source is denoted by t , and p denotes the magnitude of the (equal and opposite) momentum of each pion. The single- π^+ correlation function is

$$C_{\pi^+}(t) = \sum_{\mathbf{x}} \langle \pi^-(t, \mathbf{x}) \pi^+(0, \mathbf{0}) \rangle \quad , \quad (5)$$

where the summation over \mathbf{x} corresponds to summing over all the spatial lattice sites, thereby projecting onto the momentum $\mathbf{p} = \mathbf{0}$ state. A $\pi^+ \pi^+$ correlation function that projects onto

¹ For a nice introduction to staggered fermions and the fourth-root trick, see Ref. [63]. For the most recent discussions regarding the continuum limit of staggered fermions with the fourth-root trick, see Ref. [64, 65, 66, 67, 68, 69, 70, 71].

the s-wave state in the continuum limit is

$$C_{\pi^+\pi^+}(p, t) = \sum_{|\mathbf{p}|=p} \sum_{\mathbf{x}, \mathbf{y}} e^{i\mathbf{p}\cdot(\mathbf{x}-\mathbf{y})} \langle \pi^-(t, \mathbf{x}) \pi^-(t, \mathbf{y}) \pi^+(0, \mathbf{0}) \pi^+(0, \mathbf{0}) \rangle , \quad (6)$$

where, in eqs. (5) and (6), $\pi^+(t, \mathbf{x}) = \bar{u}(t, \mathbf{x})\gamma_5 d(t, \mathbf{x})$ is an interpolating field (Gaussian-smearing) for the π^+ . In the relatively large lattice volumes that we are using, the energy difference between the interacting and non-interacting two-meson states is a small fraction of the total energy, which is dominated by the masses of the mesons. In order to extract this energy difference we formed the ratio of correlation functions, $G_{\pi^+\pi^+}(p, t)$, where

$$G_{\pi^+\pi^+}(p, t) \equiv \frac{C_{\pi^+\pi^+}(p, t)}{C_{\pi^+}(t)C_{\pi^+}(t)} \rightarrow \sum_{n=0}^{\infty} \mathcal{A}_n e^{-\Delta E_n t} , \quad (7)$$

and the arrow denotes the large-time behavior of $G_{\pi^+\pi^+}$ in the absence of boundaries on the lattice and becomes an equality in the limit of an infinite number of gauge configurations. In $G_{\pi^+\pi^+}$, some of the fluctuations that contribute to both the one- and two-meson correlation functions cancel, thereby improving the quality of the extraction of the energy difference beyond what we are able to achieve from an analysis of the individual correlation functions.

The energy eigenvalue E_n and its deviation from the sum of the rest masses of the particle, ΔE_n , are related to the center-of-mass momentum p_n by

$$\Delta E_n \equiv E_n - 2m_\pi = 2\sqrt{p_n^2 + m_\pi^2} - 2m_\pi . \quad (8)$$

In the absence of interactions between the particles, $|p \cot \delta| = \infty$, and the energy levels occur at momenta $\mathbf{p} = 2\pi\mathbf{j}/L$, corresponding to single-particle modes in a cubic volume. In the interacting theory, once the energy shift has been computed, the real part of the inverse scattering amplitude is determined via the Lüscher formula [18, 19, 20, 21]. To obtain $p \cot \delta(p)$, where $\delta(p)$ is the phase shift, the magnitude of the center-of-mass momentum, p , is extracted from the energy shift, given in eq. (8), and inserted into [18, 19, 20, 21, 22]:

$$p \cot \delta(p) = \frac{1}{\pi L} \mathbf{S} \left(\frac{pL}{2\pi} \right) , \quad (9)$$

which is valid below the inelastic threshold. The regulated three-dimensional sum is [22]

$$\mathbf{S}(\eta) \equiv \sum_{\mathbf{j}}^{\|\mathbf{j}\| < \Lambda} \frac{1}{|\mathbf{j}|^2 - \eta^2} - 4\pi\Lambda , \quad (10)$$

where the summation is over all triplets of integers \mathbf{j} such that $\|\mathbf{j}\| < \Lambda$ and the limit $\Lambda \rightarrow \infty$ is implicit. The approximate formula [18, 19, 20, 21] that can be used for $L \gg a$ is

$$\Delta E_0 = -\frac{4\pi a}{m_\pi L^3} \left[1 + c_1 \frac{a}{L} + c_2 \left(\frac{a}{L} \right)^2 \right] + \mathcal{O} \left(\frac{1}{L^6} \right) , \quad (11)$$

which relates the ground-state energy shift to the phase shift, with

$$c_1 = \frac{1}{\pi} \sum_{\mathbf{j} \neq \mathbf{0}}^{\|\mathbf{j}\| < \Lambda} \frac{1}{|\mathbf{j}|^2} - 4\Lambda = -2.837297 , \quad c_2 = c_1^2 - \frac{1}{\pi^2} \sum_{\mathbf{j} \neq \mathbf{0}} \frac{1}{|\mathbf{j}|^4} = 6.375183 , \quad (12)$$

and a is the scattering length, defined by

$$a = \lim_{p \rightarrow 0} \frac{\tan \delta(p)}{p} . \quad (13)$$

For the $I = 2$ $\pi\pi$ scattering length that we compute here, the difference between the exact solution and the approximate solution in eq. (11) is $\lesssim 1\%$. For the volumes we consider (with $L \simeq 2.5$ fm), the center-of-mass momentum is obviously non-zero and therefore one should keep in mind the effective range expansion:

$$p \cot \delta(p) = \frac{1}{a} + \frac{1}{2} r p^2 + \mathcal{O}(p^4) , \quad (14)$$

where r is the effective range, which appears at $\mathcal{O}(1/L^6)$ in eq. (11), and include the truncation of eq. (14) as a source of systematic uncertainty.

III. DATA ANALYSIS AND CHIRAL AND CONTINUUM EXTRAPOLATION

A. Results of the Lattice Calculation

It is convenient to present the results of our lattice calculation in “effective scattering length” plots, simple variants of effective-mass plots. The effective energy splitting is formed from the ratio of correlation functions

$$\Delta E_{\pi^+\pi^+}(t) = \log \left(\frac{G_{\pi^+\pi^+}(0, t)}{G_{\pi^+\pi^+}(0, t+1)} \right) , \quad (15)$$

which in the limit of an infinite number of gauge configurations would become a constant at large times that is equal to the lowest energy of the interacting π^+ 's in the volume. At each time-slice, $\Delta E_{\pi^+\pi^+}(t)$ is inserted into eq. (9) (or eq. (11)), to give a scattering length at each time slice, $a_{\pi^+\pi^+}(t)$. It is customary to consider the dimensionless quantity given by the pion mass times the scattering length, $m_\pi a_{\pi^+\pi^+}$, where $m_\pi(t)$ is the pion effective mass, in order to remove scale-setting uncertainties. For each of the MILC ensembles that we analyze, the effective scattering lengths are shown in fig. 1. The statistical uncertainty at each time slice has been generated with the Jackknife procedure. The values of the pion masses, decay constants and $\pi\pi$ energy-shifts that we have calculated are shown in Table II.

B. Two-Flavor Mixed-Action χ -PT at One Loop

The mixed-action corrections for the $I = 2$ $\pi\pi$ scattering length have been determined in Ref. [45]. It was demonstrated that when the extrapolation formulae for this system are expressed in terms of the lattice-physical parameters ² as computed on the lattice, m_π , and f_π ,

² We denote quantities that are computed directly from the correlation functions, such as m_π , as lattice-physical quantities. These are not extrapolated to the continuum, to infinite-volume or to the physical point.

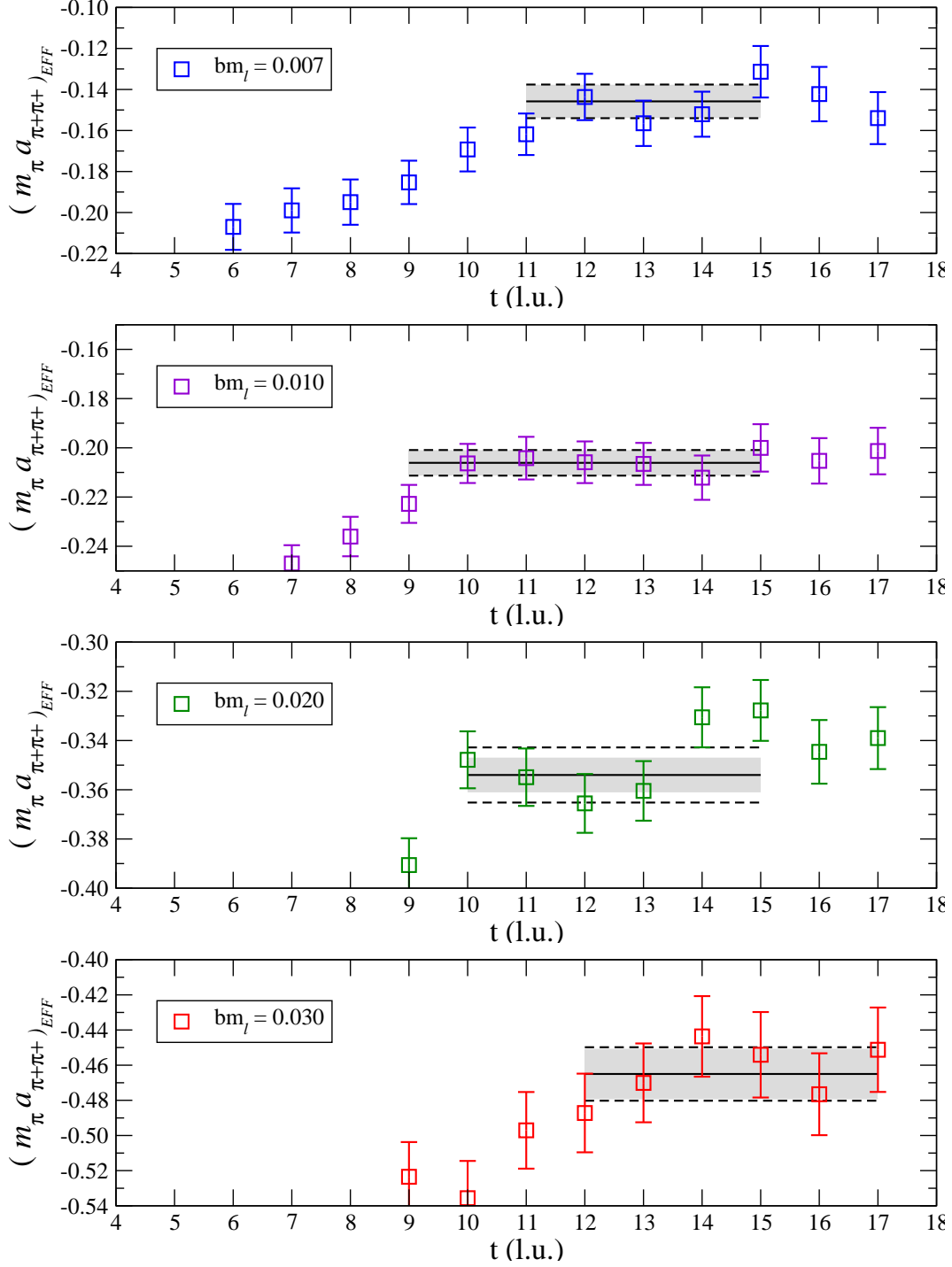


FIG. 1: The effective $\pi^+\pi^+$ scattering length times the effective π mass as a function of time slice arising from smeared sinks. The solid black lines and shaded regions are fits with $1\text{-}\sigma$ statistical uncertainties tabulated in Table II. The dashed lines are estimates of the systematic uncertainty due to fitting, also given in Table II.

there are no lattice-spacing-dependent counterterms at $\mathcal{O}(b^2)$, $\mathcal{O}(b^4)$ or $\mathcal{O}(m_\pi^2 b^2) \sim \mathcal{O}(b^4)$. This was explained to be a general feature of the two-meson systems at this order, including

TABLE II: The summary table of raw fit quantities required for the two-flavor analysis. The first uncertainties are statistical, the second uncertainties are systematic uncertainties due to fitting and the third uncertainty, when present, is a comprehensive systematic uncertainty, as discussed in the text.

Quantity	$m_l = 0.007$	$m_l = 0.010$	$m_l = 0.020$	$m_l = 0.030$
Fit Range	8 – 12	8 – 13	7 – 13	9 – 12
m_π (l.u.)	0.18454(58)(51)	0.22294(31)(09)	0.31132(28)(21)	0.37407(49)(12)
f_π (l.u.)	0.09273(29)(42)	0.09597(16)(10)	0.10179(12)(28)	0.10759(28)(17)
m_π/f_π	1.990(11)(14)	2.3230(57)(30)	3.0585(49)(95)	3.4758(98)(60)
Fit Range	11 – 15	9 – 15	10 – 15	12 – 17
$\Delta E_{\pi\pi}$ (l.u.)	0.00779(47)(14)	0.00745(20)(07)	0.00678(18)(20)	0.00627(23)(10)
$m_\pi a_{\pi\pi}^{I=2} (b \neq 0)$	-0.1458(78)(25)(14)	-0.2061(49)(17)(20)	-0.3540(68)(89)(35)	-0.465(14)(06)(05)
$l_{\pi\pi}^{I=2} (b \neq 0)$	6.1(1.9)(0.7)(0.4)	5.23(68)(24)(28)	6.53(32)(42)(16)	6.90(40)(18)(13)
$\delta (b \neq 0)$ (degrees)	-1.71(14)(04)	-2.181(81)(28)	-3.01(09)(12)	-3.46(17)(07)
$ \mathbf{p} /m_\pi$	0.2032(60)(18)	0.1836(25)(09)	0.1480(17)(23)	0.1298(24)(10)

TABLE III: Summary table for fit quantities extrapolated to the continuum with two-flavor MA χ PT. The first row corresponds to the overall mixed action correction to the scattering length. The uncertainties are discussed in detail in Section IV. The second and third rows are the continuum limit scattering length and low-energy constant. The first uncertainties are statistical and the second uncertainties are comprehensive systematic uncertainties.

Quantity	$m_l = 0.007$	$m_l = 0.010$	$m_l = 0.020$	$m_l = 0.030$
$\Delta (m_\pi a_{\pi\pi}^{I=2})$	0.0033(02)(02)(32)(55)	0.0030(02)(04)(35)(22)	0.0023(01)(10)(36)(03)	0.0018(01)(16)(32)(01)
$m_\pi a_{\pi\pi}^{I=2} (b \rightarrow 0)$	-0.1491(78)(32)	-0.2091(49)(34)	-0.356(07)(11)	-0.467(14)(09)
$l_{\pi\pi}^{I=2} (b \rightarrow 0)$	5.3(1.9)(1.8)	4.83(68)(73)	6.42(32)(51)	6.85(40)(27)

the non-zero momentum states [46]. There are additional lattice-spacing corrections due to the hairpin interactions present in mixed-action theories, but for our scheme of domain-wall valence propagators calculated in the background of the asqtad improved MILC gauge configurations, these contributions are completely calculable without additional counterterms at NLO, as they depend only upon valence meson masses and the staggered taste-identity meson mass splitting [45, 46] which has been computed [15]. This allows us to precisely determine the predicted mixed-action corrections for the scattering lengths at the various pion masses used in this work. In two-flavor MA χ -PT (i.e. including finite lattice-spacing corrections) the chiral expansion of the scattering length at NLO takes the form [46]

$$m_\pi a_{\pi\pi}^{I=2}(b \neq 0) = -\frac{m_\pi^2}{8\pi f_\pi^2} \left\{ 1 + \frac{m_\pi^2}{16\pi^2 f_\pi^2} \left[3 \log \left(\frac{m_\pi^2}{\mu^2} \right) - 1 - l_{\pi\pi}^{I=2}(\mu) - \frac{\tilde{\Delta}_{ju}^4}{6m_\pi^4} \right] \right\}, \quad (16)$$

where it is understood that m_π and f_π are the lattice-physical parameters [46] and

$$\tilde{\Delta}_{ju}^2 \equiv \tilde{m}_{jj}^2 - m_{uu}^2 = 2B_0(m_j - m_u) + b^2\Delta_I + \dots, \quad (17)$$

where u denotes a valence quark and j denotes a sea-quark, and we are using isospin-symmetric sea and valence quarks. \tilde{m}_{jj} (m_{uu}) is the mass of a meson composed of two sea (valence) quarks of mass m_j (m_u) and the dots denote higher-order corrections to the meson masses. Clearly eq. (16), which contains all $\mathcal{O}(m_\pi^2 b^2)$ and $\mathcal{O}(b^4)$ lattice artifacts, reduces to

the continuum expression for the scattering length [2] in the QCD limit where $\tilde{\Delta}_{ju}^2 \rightarrow 0$ ³. It is worth noting that eq. (16), and the subsequent expression for the three-flavor theory, become the partially-quenched formulae in the continuum limit. Therefore, they are the correct extrapolation formulae to use in the case of non-degenerate valence- and sea-quark masses, as is implied by eq. (16) and eq. (17). This modification of the partially-quenched formulae can be understood on more general grounds, as mixed-action theories with chirally-symmetric valence fermions exhibit many universal features [72].

With domain-wall fermion masses tuned to match the staggered Goldstone pion [47, 48], one finds $\tilde{\Delta}_{ju}^2 = b^2 \Delta_I$. The various fit parameters relevant to the two-flavor extrapolation are presented in Table II. For each ensemble we determine $m_\pi a_{\pi\pi}^{I=2}$, and then use the chiral extrapolation formula to extract a value of the counterterm $l_{\pi\pi}^{I=2}(\mu = f_\pi)$, with a statistical uncertainty determined with the Jackknife procedure. The systematic uncertainties are propagated through in quadrature. The results of the two-flavor extrapolation to the continuum are shown in Table III.

Fitting to lattice data at the lightest accessible values of the quark masses will optimize the convergence of the chiral expansion. While we only have four different quark masses in our data set, with pion masses, $m_\pi \sim 290$ MeV, 350 MeV, 490 MeV and 590 MeV, fitting all four data sets and then “pruning” the heaviest data set and refitting provides a useful measure of the convergence of the chiral expansion. Hence, in “fit A”, we fit the $l_{\pi\pi}^{I=2}(\mu = f_\pi)$ ’s extracted from all four lattice ensembles (m007, m010, m020 and m030) to a constant, while in “fit B”, we fit the $l_{\pi\pi}^{I=2}(\mu = f_\pi)$ ’s from the lightest three lattice ensembles (m007, m010 and m020). In “fit C”, we fit the $l_{\pi\pi}^{I=2}(\mu = f_\pi)$ ’s from the lightest two lattice ensembles (m007 and m010). Results are given in Table IV.

TABLE IV: Results of the fits in two-flavor Mixed-Action χ -PT. The values of $m_\pi a_{\pi\pi}^{I=2}$ correspond to the extrapolated values at the physical point. The first uncertainty is statistical and the second is a comprehensive systematic uncertainty.

FIT	$l_{\pi\pi}^{I=2}(\mu = f_\pi)$	$m_\pi a_{\pi\pi}^{I=2}$ (extrapolated)	χ^2/dof
A	$6.43 \pm 0.23 \pm 0.26$	$-0.043068 \pm 0.000076 \pm 0.000085$	1.17
B	$5.97 \pm 0.29 \pm 0.42$	$-0.043218 \pm 0.00009 \pm 0.00014$	0.965
C	$4.89 \pm 0.64 \pm 0.68$	$-0.04357 \pm 0.00021 \pm 0.00022$	0.054

Taking the range of parameters spanned by fits A-C one finds:

$$\begin{aligned}
 l_{\pi\pi}^{I=2}(\mu = f_\pi) &= 5.4 \pm 1.4 \\
 m_\pi a_{\pi\pi}^{I=2} &= -0.04341 \pm 0.00046 .
 \end{aligned}
 \tag{18}$$

In Fig. 2 we show the results of our calculation, along with the lowest mass $n_f = 2$ point from CP-PACS (not included in our fit). We also show the tree-level prediction and the results of our two-flavor fit described in this section. The experimental point shown in Fig. 2 is not included in the fit and extrapolation. It is interesting that the lattice data indicates little deviation from the tree level χ PT curve. The significant deviation of the extrapolated scattering length from the tree-level result is entirely a consequence of fitting to MA χ PT at one-loop level.

³ The counterterm $l_{\pi\pi}^{I=2}(\mu)$ is, of course, the same counterterm that appears in continuum χ PT.

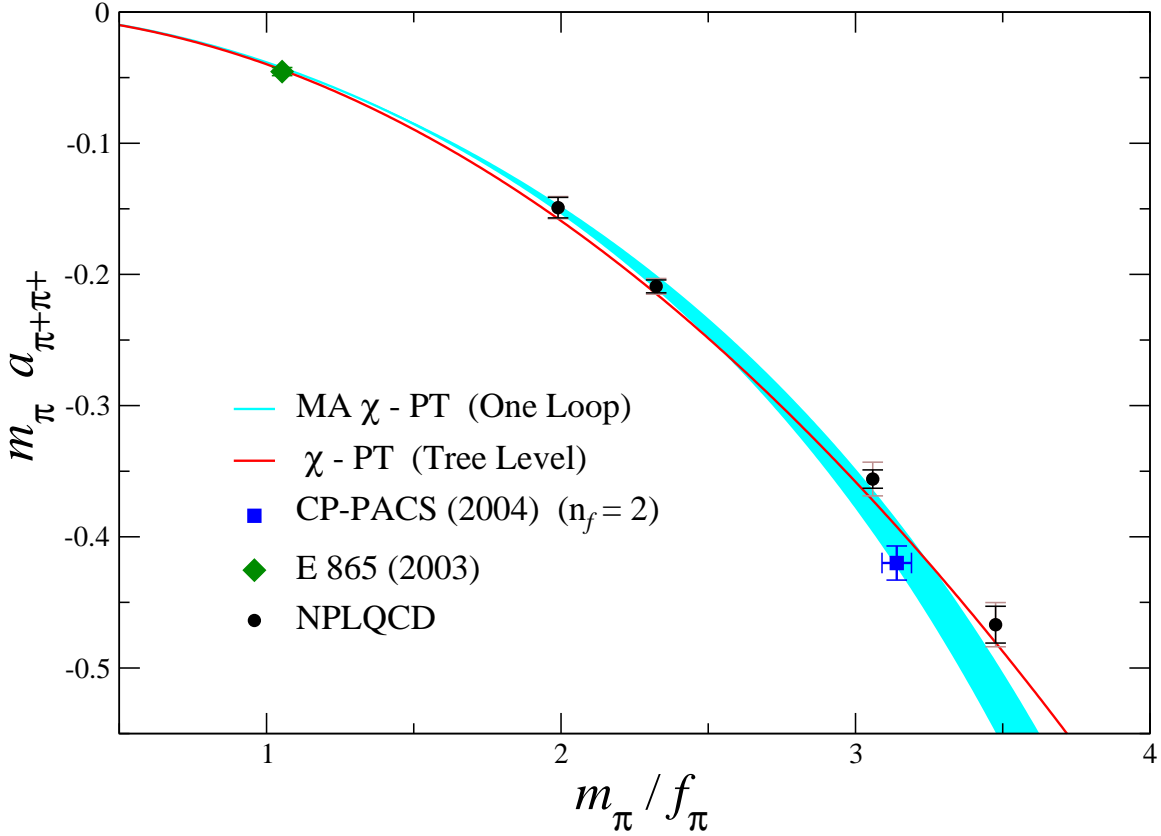


FIG. 2: $m_\pi a_{\pi\pi}^{I=2}$ vs. m_π/f_π (ovals) with statistical (dark bars) and systematic (light bars) uncertainties. Also shown are the experimental value from Ref. [6] (diamond) and the lowest quark mass result of the $n_f = 2$ dynamical calculation of CP-PACS [43] (square). The blue band corresponds to a weighted fit to the lightest three data points (fit B) using the one-loop MA χ -PT formula in eq. (16) (the shaded region corresponds only to the statistical uncertainty). The red line is the tree-level χ -PT result. The experimental data is not used in the chiral extrapolation fits.

C. Three-Flavor Mixed-Action χ -PT at One Loop

An important check of the systematic uncertainties involved in the chiral extrapolation is to perform the same analysis using three-flavor MA χ -PT [45, 46] as both the real world and our lattice calculation have three active light flavors. In addition to the computations presented in Table II, it is necessary to determine masses and decay constants for the kaon and the η . We use the Gell-Mann–Okubo mass-relation among the mesons to determine the η mass, which we do not compute in this lattice calculation due the enormous computer resources (beyond what is available to us) required to compute the disconnected contributions. This procedure is consistent to the order in the chiral expansion to which we are working.

The chiral expansion of the $\pi^+\pi^+$ scattering length in three-flavor mixed-action χ PT

TABLE V: The summary table of quantities required for the three-flavor analysis. A “ * ” denotes that the Gell-Mann-Okubo mass relation among the mesons has been used to determine this quantity. The first uncertainties are statistical and the second are systematic (that are discussed in the text).

Quantity	$m_l = 0.007$	$m_l = 0.010$	$m_l = 0.020$	$m_l = 0.030$
Fit Range	8 – 14	9 – 14	9 – 13	9 – 13
m_K (l.u.)	0.36839(40)(29)	0.37797(30)(03)	0.40540(31)(32)	0.42976(41)(20)
m_η (l.u.) *	0.41182(43)(36)	0.41703(32)(04)	0.43224(33)(46)	0.44688(38)(26)
m_η/f_π *	4.447(19)(20)	4.3517(96)(43)	4.246(06)(12)	4.154(11)(05)
\tilde{m}_X/f_π *	5.408(23)(24)	5.271(11)(05)	5.087(07)(14)	4.927(13)(06)
Σ *	-0.0015(01)	-0.0027(00)	-0.0079(01)	-0.0130(03)
Γ *	0.0011(01)	0.0003(01)	-0.0012(01)	-0.0018(01)
$m_\pi a_{\pi\pi}^{I=2} (b \rightarrow 0)$ *	-0.1470(78)(70)	-0.2065(49)(50)	-0.353(07)(10)	-0.462(14)(08)
$32(4\pi)^2 L_{\pi\pi}^{I=2}$ *	6.4(1.9)(1.7)	5.66(67)(68)	7.07(32)(48)	7.44(40)(21)

takes the form [46]:

$$m_\pi a_{\pi\pi}^{I=2}(b \neq 0) = -\frac{m_\pi^2}{8\pi f_\pi^2} \left\{ 1 + \frac{m_\pi^2}{16\pi^2 f_\pi^2} \left[3 \log \left(\frac{m_\pi^2}{\mu^2} \right) - 32(4\pi)^2 L_{\pi\pi}^{I=2}(\mu) + \frac{1}{9} \log \left(\frac{\tilde{m}_X^2}{\mu^2} \right) - \frac{8}{9} - \frac{\tilde{\Delta}_{ju}^4}{6m_\pi^4} + \sum_{n=1}^4 \left(\frac{\tilde{\Delta}_{ju}^2}{m_\pi^2} \right)^n \mathcal{F}_n \left(\frac{m_\pi^2}{\tilde{m}_X^2} \right) \right] \right\}, \quad (19)$$

where $\tilde{m}_X^2 = m_\eta^2 + b^2 \Delta_I$, and

$$\begin{aligned} \mathcal{F}_1(y) &= -\frac{2y}{9(1-y)^2} [5(1-y) + (3+2y) \ln(y)], \\ \mathcal{F}_2(y) &= \frac{2y}{3(1-y)^3} [(1-y)(1+3y) + y(3+y) \ln(y)], \\ \mathcal{F}_3(y) &= \frac{y}{9(1-y)^4} [(1-y)(1-7y-12y^2) - 2y^2(7+2y) \ln(y)], \\ \mathcal{F}_4(y) &= -\frac{y^2}{54(1-y)^5} [(1-y)(1-8y-17y^2) - 6y^2(3+y) \ln(y)]. \end{aligned} \quad (20)$$

In addition, it is useful to define the quantities:

$$\Gamma \equiv -\frac{2\pi m_\pi^4}{(4\pi f_\pi)^4} \left[-\frac{\tilde{\Delta}_{ju}^4}{6m_\pi^4} + \sum_{n=1}^4 \left(\frac{\tilde{\Delta}_{ju}^2}{m_\pi^2} \right)^n \mathcal{F}_n \left(\frac{m_\pi^2}{\tilde{m}_X^2} \right) \right] \quad (21)$$

and

$$\Sigma \equiv -\frac{m_\pi^2}{8\pi f_\pi^2} \frac{m_\pi^2}{16\pi^2 f_\pi^2} \frac{1}{9} \log \left(\frac{\tilde{m}_X^2}{f_\pi^2} \right), \quad (22)$$

whose numerical values for the various ensembles are given in Table V.

For the three-flavor analysis, we follow the same procedure of “pruning” the data as in the two-flavor analysis, giving the results shown in Table VI. Taking the range of parameters spanned by fits D-F one finds:

$$\begin{aligned} 32(4\pi) L_{\pi\pi}^{I=2}(\mu = f_\pi) &= 6.2 \pm 1.2 \\ m_\pi a_{\pi\pi}^{I=2} &= -0.04330 \pm 0.00042 \quad . \end{aligned} \quad (23)$$

TABLE VI: Results of the NLO fits in three-flavor Mixed-Action χ -PT. The values of $m_\pi a_{\pi\pi}^{I=2}$ correspond to the extrapolated values at the physical point. The first uncertainty is statistical and the second is a comprehensive systematic uncertainty.

FIT	$32(4\pi)L_{\pi\pi}^{I=2}(\mu = f_\pi)$	$m_\pi a_{\pi\pi}^{I=2}$ (extrapolated)	χ^2/dof
D	$7.09 \pm 0.23 \pm 0.23$	$-0.042992 \pm 0.000076 \pm 0.000077$	0.969
E	$6.69 \pm 0.29 \pm 0.39$	$-0.04312 \pm 0.00009 \pm 0.00013$	0.803
F	$5.75 \pm 0.63 \pm 0.64$	$-0.04343 \pm 0.00021 \pm 0.00021$	0.073

TABLE VII: Corrections and uncertainties in $m_\pi a_{\pi\pi}^{I=2}$ for $n_f = 2$.

Quantity	$m_l = 0.007$	$m_l = 0.010$	$m_l = 0.020$	$m_l = 0.030$
$\Delta_{MA} \left(m_\pi a_{\pi\pi}^{I=2} \right)$	0.0033(02)(02)	0.0030(02)(04)	0.0023(01)(10)	0.0018(01)(16)
$\Delta_{FV} \left(m_\pi a_{\pi\pi}^{I=2} \right)$	± 0.0055	± 0.0022	± 0.0003	± 0.0001
$\Delta_{m_{res}} \left(m_\pi a_{\pi\pi}^{I=2} \right)$	± 0.0032	± 0.0035	± 0.0036	± 0.0032

IV. SYSTEMATIC UNCERTAINTIES

This section describes the sources of systematic uncertainty that need to be quantified.

A. Higher-Order Effects in Mixed-Action χ -PT

We rely on the power counting associated with the chiral expansion of the Mixed-Action χ PT to estimate the size of the lattice-spacing artifacts arising at $\mathcal{O}(m_\pi^4 b^2)$. To be conservative, we have estimated these corrections to be of the general size

$$\mathcal{O}(m_\pi^4 b^2) \sim \frac{2\pi m_\pi^4}{(4\pi f_\pi)^4} \frac{b^2 \Delta_I}{(4\pi f_\pi)^2} . \quad (24)$$

We treat these estimates as uncertainties in the predicted NLO MA χ PT corrections which can be determined from eq. (16) and eq. (19). We provide these predicted corrections and their uncertainties in the form

$$\Delta_{MA} \left(m_\pi a_{\pi\pi}^{I=2} \right) = m_\pi a_{\pi\pi}^{I=2} \Big|_{MA} - m_\pi a_{\pi\pi}^{I=2} \Big|_{\chi PT} . \quad (25)$$

The values of these corrections are shown in Tables VII and VIII. The first uncertainty in these corrections is statistical and is associated with the meson masses, decay constants and the taste-identity mass splitting, $b^2 \Delta_I$. The second uncertainty is the power counting estimate of the higher-order corrections of $\mathcal{O}(m_\pi^4 b^2)$ as estimated in eq. (24). The calculable corrections to $m_\pi a_{\pi\pi}^{I=2}$ at $\mathcal{O}(m_\pi^2 b^2, b^4)$ are 2.3%, 1.5%, 0.65% and 0.39% effects for the 007, 010, 020 and 030 ensembles, respectively, from which we conclude that the $\mathcal{O}(m_\pi^4 b^2)$ contributions are significantly less than $\sim 1\%$.

TABLE VIII: Corrections and uncertainties in $m_\pi a_{\pi\pi}^{I=2}$ for $n_f = 2 + 1$.

Quantity	$m_l = 0.007$	$m_l = 0.010$	$m_l = 0.020$	$m_l = 0.030$
$\Delta_{MA} \left(m_\pi a_{\pi\pi}^{I=2} \right)$	0.0012(01)(02)	0.0004(01)(04)	-0.0015(03)(10)	-0.0027(05)(16)
$\Delta_{FV} \left(m_\pi a_{\pi\pi}^{I=2} \right)$	± 0.0024	± 0.0005	± 0.0001	± 0.00006
$\Delta_{m_{res}} \left(m_\pi a_{\pi\pi}^{I=2} \right)$	± 0.0032	± 0.0035	± 0.0036	± 0.0032

B. Finite-Volume Effects in Mixed-Action χ -PT

The universal relation between the two-particle energy levels in a finite volume and their infinite-volume scattering parameters receives non-universal corrections which are exponentially suppressed by the lattice size and dominated by the lightest particle in the spectrum. These scale generically as $e^{-m_\pi L}$ [73, 74]. In Ref. [75], the leading exponential volume corrections to $p \cot \delta(p)$ were determined in the $I = 2$ $\pi\pi$ scattering channel in χ PT. However, in order to determine the leading finite-volume corrections to this mixed-action calculation, hairpin diagrams present in the mixed-action theory must also be included. For the $I = 2$ $\pi\pi$ system, there are additional hairpin diagrams present in the t and u channel scattering diagrams [45]. The finite-volume corrections from these diagrams are larger than those in continuum χ PT, but are opposite in sign and therefore the overall magnitude of the correction is similar to that given in Ref. [75]. We note that as these contributions vanish in the continuum limit, they are actually finite-volume finite-lattice-spacing corrections, and not just finite-volume corrections, and hence scale as $b^2 \exp(-m_\pi L)$ at small lattice spacing.

As with the mixed-action lattice-spacing corrections, we denote these finite-volume modifications as

$$\Delta_{FV} \left(m_\pi a_{\pi\pi}^{I=2} \right) = m_\pi a_{\pi\pi}^{I=2} \Big|_{FV} - m_\pi a_{\pi\pi}^{I=2} \Big|_{\infty V}, \quad (26)$$

and they are shown in Tables VII and VIII. However, one should take note that the effective-range contribution to $p \cot \delta(p)$, which behaves as a power-law in the lattice size (and therefore is parametrically enhanced over the exponential corrections) is not included in the extraction of the scattering lengths. While the exponential modifications are numerically larger than our estimate of the effective-range contributions at the light pion masses (see below), the values of $\Delta_{FV}(m_\pi a_{\pi\pi}^{I=2})$ shown in Tables VII and VIII are used as estimates of the uncertainties due to higher-order finite-volume effects.

C. Residual Chiral Symmetry Breaking

The mixed-action formulae describing $\pi\pi$ scattering determined in Refs. [45, 46] have assumed that the valence fermions have exact chiral symmetry, up to the quark-mass corrections. The domain-wall propagators used in this work have a finite fifth-dimensional extent and therefore residual chiral symmetry breaking arising from the overlap of the left- and right-handed quark fields bound to the opposite domain walls. Due to the nature of this residual chiral symmetry breaking in the domain-wall action, the leading contributions can be parameterized as an additive shift to the valence-quark masses [60, 62],

$$m_l^{dwf} \rightarrow m_l^{dwf} + m_{res}. \quad (27)$$

A full treatment of these effects involves three new spurion fields in the effective field theory [76] but this is not necessary for estimating the size of these contributions to the $\pi\pi$ scattering lengths. By expressing the calculated scattering lengths and extrapolation formulae in terms of the lattice-physical meson masses and decay constants, the dominant contributions from residual chiral symmetry breaking are included, leaving corrections at higher orders in the chiral expansion. There will be new operators similar to the Gasser-Leutwyler operators [77] in the chiral Lagrangian, for example

$$\begin{aligned} \bar{\mathcal{L}} = & 2B_0 \bar{L}_4 \operatorname{str} \left(\partial_\mu \Sigma \partial^\mu \Sigma^\dagger \right) \operatorname{str} \left(m_{res} \Sigma^\dagger + \Sigma m_{res}^\dagger \right) \\ & + 8B_0^2 \bar{L}_6 \operatorname{str} \left(m_q \Sigma^\dagger + \Sigma m_q^\dagger \right) \operatorname{str} \left(m_{res} \Sigma^\dagger + \Sigma m_{res}^\dagger \right) + \dots \end{aligned} \quad (28)$$

Naive dimensional analysis [78] can be used to estimate the size of the corrections due to these new operators, which in the case of the $I = 2$ $\pi\pi$ system are given by

$$\Delta_{m_{res}}(m_\pi a_{\pi\pi}^{I=2}) = \frac{8\pi m_\pi^4}{(4\pi f_\pi)^4} \frac{m_{res}}{m_l} . \quad (29)$$

There will be additional operators with two insertions of m_{res} in the place of m_q , but these are $\lesssim 20\%$ of the uncertainty already estimated for the residual chiral symmetry breaking. These uncertainties are denoted by

$$\Delta_{m_{res}}(m_\pi a_{\pi\pi}^{I=2}) = m_\pi a_{\pi\pi}^{I=2} \Big|_{m_{res}} - m_\pi a_{\pi\pi}^{I=2} \Big|_{m_{res}=0} , \quad (30)$$

and are shown in Tables VII and VIII.

D. Two Loops Effects

The two-loop expression for the scattering length [4, 9] is given, in the continuum limit of QCD, by

$$\begin{aligned} m_\pi a_{\pi\pi}^{I=2} = & -\frac{m_\pi^2}{8\pi f_\pi^2} \left\{ 1 + \frac{m_\pi^2}{16\pi^2 f_\pi^2} \left[3 \log \frac{m_\pi^2}{\mu^2} - 1 - l_{\pi\pi}^{I=2}(\mu) \right] \right. \\ & \left. + \frac{m_\pi^4}{64\pi^4 f_\pi^4} \left[\frac{31}{6} \left(\log \frac{m_\pi^2}{\mu^2} \right)^2 + l_{\pi\pi}^{(2)}(\mu) \log \frac{m_\pi^2}{\mu^2} + l_{\pi\pi}^{(3)}(\mu) \right] \right\} , \end{aligned} \quad (31)$$

where $l_{\pi\pi}^{(2)}$ and $l_{\pi\pi}^{(3)}$ are linear combinations of undetermined constants that appear in the $\mathcal{O}(p^4)$ and $\mathcal{O}(p^6)$ chiral Lagrangians [2, 4]. Fitting all four data points allows for an extraction of the three counterterms with $\chi^2/\text{dof} = 0.26$. From the 68% confidence-interval error ellipsoid we find an extrapolated value of:

$$m_\pi a_{\pi\pi}^{I=2} = -0.0442 \pm 0.0030 . \quad (32)$$

While it is gratifying to have a determination of the scattering length at two-loop level that is consistent with the one-loop result, there are several caveats: i) the two-loop expression in MA χ -PT does not yet exist and therefore the determination in eq. (31) contains lattice-spacing artifacts at lower orders in the chiral expansion than in the one-loop result; ii) This value is clearly strongly dependent on the heaviest quark mass, which is, at best, at the boundary of the range of validity of the chiral expansion. A reliable two-loop determination will have to await further lattice data at quark masses closer to the chiral limit than we currently possess.

E. Range Corrections

It is straightforward to show that the range corrections enter at $\mathcal{O}(L^{-6})$ in eq. (11). Assuming that the effective range is of order the scattering length (the scattering length is of natural size), we expect a fractional uncertainty of $(m_\pi a)^2 p^2 / 2m_\pi^2$ due to the omission of range corrections. For the ensembles that we consider, this translates into an 0.5% uncertainty in $m_\pi a_{\pi\pi}^{I=2}$. Allowing for the effective range to exceed its natural value by a factor of two, we assign a 1% systematic uncertainty to $m_\pi a_{\pi\pi}^{I=2}$ determined on each ensemble.

F. Isospin Violation

The calculation we have performed is in the limit of exact isospin symmetry, as are the extrapolation formula we have used to analyze the results. The conventional discussion of the scattering length is in the unphysical theory with $e = 0$ and $m_u = m_d = m$, with $m_\pi = m_{\pi^+} = 139.57018 \pm 0.00035$ MeV and $f_\pi = f_{\pi^+} = 130.7 \pm 0.14 \pm 0.37$ MeV. Hence $m_{\pi^+}/f_{\pi^+} = 1.0679 \pm 0.0032$, where the statistical and systematic uncertainties have been combined in quadrature. We extrapolate the results of our lattice calculations to this value.

Unfortunately, we are presently unable to make precise predictions for the real world in which isospin breaking occurs at the few-percent level. Extrapolation to the isospin-averaged pion mass (as opposed to the charged pion mass), would introduce a shift of $\sim 2\%$ in $m_\pi a_{\pi\pi}^{I=2}$. This is larger than the uncertainty we have determined at the charged pion mass. It is clear that in order to make predictions for real-world quantities at the $\sim 1\%$ level from lattice QCD calculations, isospin-breaking and electromagnetism will need to be incorporated into the lattice calculation.

V. DISCUSSION

We have presented results of a lattice QCD calculation of the $I = 2$ $\pi\pi$ scattering length performed with domain-wall valence quarks on asqtad-improved MILC configurations with 2+1 dynamical staggered quarks. The calculations were performed at a single lattice spacing of $b \sim 0.125$ fm and at a single lattice spatial size of $L \sim 2.5$ fm with four values of the light quark masses, corresponding to pion masses of $m_\pi \sim 290, 350, 490$ MeV and 590 MeV. High statistics were generated by computing up to twenty-four propagators per MILC configuration at spatially- and temporally-displaced sources. We used one-loop $\text{MA}\chi\text{-PT}$ with two and three flavors of light quarks to perform the chiral and continuum extrapolations. Our prediction for the physical value of the $I = 2$ $\pi\pi$ scattering length is $m_\pi a_{\pi\pi}^{I=2} = -0.04330 \pm 0.00042$, which agrees within uncertainties with the (non-lattice) determination of CGL [9], but we emphasize once again that our result rests on the assumption that the fourth-root trick recovers the correct continuum limit of QCD. In Table IX and fig. 3 we offer a comparison of our prediction with other determinations. What has enabled such an improvement in precision over our previous result on the coarse MILC lattices is the recent understanding of the lattice-spacing artifacts accomplished with mixed-action chiral perturbation theory.

While it will be quite useful to have results at another lattice spacing and at another lattice volume, we have reached the level of precision where we require knowledge of isospin violating effects in order to further reduce the uncertainty in the physical $\pi\pi$ scattering lengths; i.e. those that can be compared to experiment. One somewhat surprising result of

TABLE IX: A compilation of the various calculations and predictions for the $I = 2$ $\pi\pi$ scattering length. The prediction made in this paper is labeled *NPLQCD (2007)*. Also included are the experimental value from Ref. [6] (*E 865 (2003)*), the previous determination by *NPLQCD [44]* (*NPLQCD (2005)*), two indirect lattice results from *MILC [15, 16]* (the stars on the *MILC* results indicate that these are not lattice calculations of the $I = 2$ $\pi\pi$ scattering length but rather a hybrid prediction which uses *MILC*'s determination of various low-energy constants together with the *Roy* equations), and the *Roy* equation determination of Ref. [9] (*CGL (2001)*).

	$m_\pi a_{\pi\pi}^{I=2}$
χ PT (Tree Level)	-0.04438
NPLQCD (2007)	-0.04330 ± 0.00042
E 865 (2003)	$-0.0454 \pm 0.0031 \pm 0.0010 \pm 0.0008$
NPLQCD (2005)	$-0.0426 \pm 0.0006 \pm 0.0003 \pm 0.0018$
MILC (2006)*	-0.0432 ± 0.0006
MILC (2004)*	-0.0433 ± 0.0009
CGL (2001)	-0.0444 ± 0.0010

our analysis is that one of the dominant sources of systematic uncertainty in our calculation is due to residual chiral symmetry breaking in the domain-wall valence quarks for the lattice parameters we have chosen. Clearly this systematic can be reduced by improving our choice of domain-wall parameters.

Lattice QCD is currently in a precision age insofar as single-particle properties are concerned. The precise prediction for the intrinsic two-particle property presented here is a remarkable demonstration of the power of combining a lattice QCD calculation with the model-independent constraints of chiral perturbation theory.

VI. ACKNOWLEDGMENTS

We thank R. Edwards for help with the QDP++/Chroma programming environment [79] with which the calculations discussed here were performed. AWL would like to thank Claude Bernard for providing a program to determine meson mass splittings in lattice units. The computations for this work were performed at Jefferson Lab, Fermilab, Lawrence Livermore National Laboratory, National Center for Supercomputing Applications, and Centro Nacional de Supercomputaci3n (Barcelona, Spain). We are indebted to the MILC and the LHP collaborations for use of their configurations and propagators, respectively. The work of MJS was supported in part by the U.S. Dept. of Energy under Grant No. DE-FG03-97ER4014. The work of KO was supported in part by the U.S. Dept. of Energy contract No. DE-AC05-06OR23177 (JSA) and contract No. DE-AC05-84150 (SURA) as well as by the Jeffress Memorial Trust, grant J-813. The work of AWL was supported in part by the U.S. Dept. of Energy grant No. DE-FG02-93ER-40762. The work of SRB and AT was supported in part by the National Science Foundation under grant No. PHY-0400231. Part of this work was performed under the auspices of the US DOE by the University of California, Lawrence Livermore National Laboratory under Contract No. W-7405-Eng-48. The work of AP was partly supported by the EU contract FLAVIANet MRTN-CT-2006-035482, by the contract FIS2005-03142 from MEC (Spain) and FEDER and by the Generalitat de

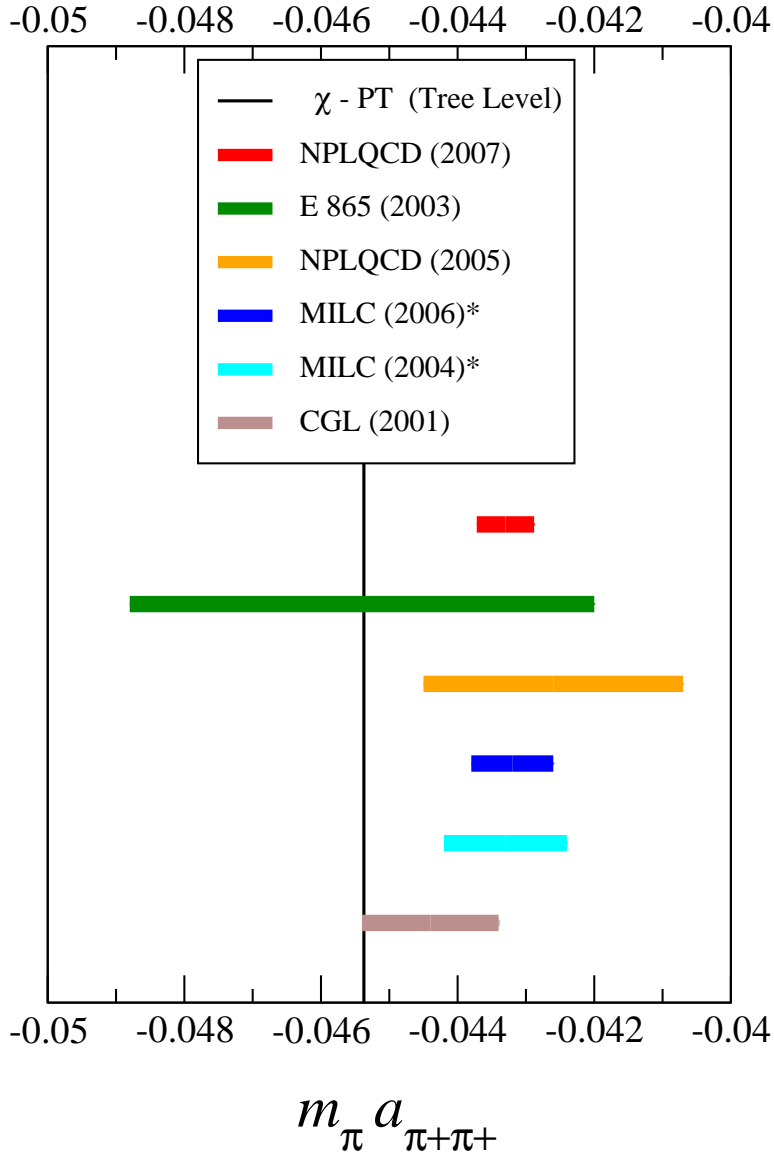


FIG. 3: Bar chart of the various determinations of the $I = 2$ $\pi\pi$ scattering length tabulated in Table IX. We reiterate that the stars on the MILC results indicate that these are not lattice calculations of the $I = 2$ $\pi\pi$ scattering length but rather a hybrid prediction which uses MILC's determination of various low-energy constants together with the Roy equations.

Catalunya contract 2005SGR-00343.

-
- [1] S. Weinberg, Phys. Rev. Lett. **17**, 616 (1966).
 - [2] J. Gasser and H. Leutwyler, Annals Phys. **158**, 142 (1984).
 - [3] J. Bijnens, G. Colangelo, G. Ecker, J. Gasser and M. E. Sainio, Phys. Lett. B **374**, 210 (1996)

- [arXiv:hep-ph/9511397];
- [4] J. Bijnens, G. Colangelo, G. Ecker, J. Gasser and M. E. Sainio, Nucl. Phys. B **508**, 263 (1997) [Erratum-ibid. B **517**, 639 (1998)] [arXiv:hep-ph/9707291].
- [5] S. Pislak *et al.* [BNL-E865 Collaboration], Phys. Rev. Lett. **87**, 221801 (2001) [arXiv:hep-ex/0106071].
- [6] S. Pislak *et al.*, Phys. Rev. D **67**, 072004 (2003) [arXiv:hep-ex/0301040].
- [7] B. Adeva *et al.* [DIRAC Collaboration], Phys. Lett. B **619**, 50 (2005) [arXiv:hep-ex/0504044].
- [8] J. R. Batley *et al.* [NA48/2 Collaboration], Phys. Lett. B **633**, 173 (2006) [arXiv:hep-ex/0511056].
- [9] G. Colangelo, J. Gasser and H. Leutwyler, Nucl. Phys. B **603**, 125 (2001) [arXiv:hep-ph/0103088].
- [10] H. Leutwyler, arXiv:hep-ph/0612112.
- [11] S. M. Roy, Phys. Lett. B **36**, 353 (1971).
- [12] J. L. Basdevant, C. D. Froggatt and J. L. Petersen, Nucl. Phys. B **72**, 413 (1974).
- [13] B. Ananthanarayan, G. Colangelo, J. Gasser and H. Leutwyler, Phys. Rept. **353**, 207 (2001) [arXiv:hep-ph/0005297].
- [14] I. Caprini, G. Colangelo and H. Leutwyler, Phys. Rev. Lett. **96**, 132001 (2006) [arXiv:hep-ph/0512364].
- [15] C. Aubin *et al.* [MILC Collaboration], Phys. Rev. D **70**, 114501 (2004) [arXiv:hep-lat/0407028].
- [16] C. Bernard *et al.* [MILC Collaboration], arXiv:hep-lat/0609053.
- [17] L. Maiani and M. Testa, Phys. Lett. B **245**, 585 (1990).
- [18] K. Huang and C. N. Yang, Phys. Rev. **105**, 767 (1957).
- [19] H. W. Hamber, E. Marinari, G. Parisi and C. Rebbi, Nucl. Phys. B **225**, 475 (1983).
- [20] M. Lüscher, Commun. Math. Phys. **105** (1986) 153.
- [21] M. Lüscher, Nucl. Phys. B **354**, 531 (1991).
- [22] S. R. Beane, P. F. Bedaque, A. Parreño and M. J. Savage, Phys. Lett. B **585**, 106 (2004) [arXiv:hep-lat/0312004].
- [23] S. R. Sharpe, R. Gupta and G. W. Kilcup, Nucl. Phys. B **383**, 309 (1992).
- [24] R. Gupta, A. Patel and S. R. Sharpe, Phys. Rev. D **48**, 388 (1993) [arXiv:hep-lat/9301016].
- [25] Y. Kuramashi, M. Fukugita, H. Mino, M. Okawa and A. Ukawa, Phys. Rev. Lett. **71**, 2387 (1993).
- [26] Y. Kuramashi, M. Fukugita, H. Mino, M. Okawa and A. Ukawa, [arXiv:hep-lat/9312016].
- [27] M. Fukugita, Y. Kuramashi, H. Mino, M. Okawa and A. Ukawa, Phys. Rev. Lett. **73**, 2176 (1994) [arXiv:hep-lat/9407012].
- [28] C. Gattringer, D. Hierl and R. Pullirsch [Bern-Graz-Regensburg Collaboration], Nucl. Phys. Proc. Suppl. **140**, 308 (2005) [arXiv:hep-lat/0409064].
- [29] M. Fukugita, Y. Kuramashi, M. Okawa, H. Mino and A. Ukawa, Phys. Rev. D **52**, 3003 (1995) [arXiv:hep-lat/9501024].
- [30] H. R. Fiebig, K. Rabitsch, H. Markum and A. Mihaly, Few Body Syst. **29**, 95 (2000) [arXiv:hep-lat/9906002].
- [31] S. Aoki *et al.* [JLQCD Collaboration], Nucl. Phys. Proc. Suppl. **83**, 241 (2000) [arXiv:hep-lat/9911025].
- [32] C. Liu, J. h. Zhang, Y. Chen and J. P. Ma, [arXiv:hep-lat/0109010].
- [33] C. Liu, J. h. Zhang, Y. Chen and J. P. Ma, Nucl. Phys. B **624**, 360 (2002) [arXiv:hep-lat/0109020].

- [34] S. Aoki *et al.* [CP-PACS Collaboration], Nucl. Phys. Proc. Suppl. **106**, 230 (2002) [arXiv:hep-lat/0110151].
- [35] S. Aoki *et al.* [JLQCD Collaboration], Phys. Rev. D **66**, 077501 (2002) [arXiv:hep-lat/0206011].
- [36] S. Aoki *et al.* [CP-PACS Collaboration], Nucl. Phys. Proc. Suppl. **119**, 311 (2003) [arXiv:hep-lat/0209056].
- [37] S. Aoki *et al.* [CP-PACS Collaboration], Phys. Rev. D **67**, 014502 (2003) [arXiv:hep-lat/0209124].
- [38] K. J. Juge [BGR Collaboration], Nucl. Phys. Proc. Suppl. **129**, 194 (2004) [arXiv:hep-lat/0309075].
- [39] N. Ishizuka and T. Yamazaki, Nucl. Phys. Proc. Suppl. **129**, 233 (2004) [arXiv:hep-lat/0309168].
- [40] S. Aoki *et al.* [CP-PACS Collaboration], [arXiv:hep-lat/0503025].
- [41] S. Aoki *et al.* [CP-PACS Collaboration], Nucl. Phys. Proc. Suppl. **140**, 305 (2005) [arXiv:hep-lat/0409063].
- [42] X. Li *et al.* [CLQCD Collaboration], arXiv:hep-lat/0703015.
- [43] T. Yamazaki *et al.* [CP-PACS Collaboration], Phys. Rev. D **70**, 074513 (2004) [arXiv:hep-lat/0402025].
- [44] S. R. Beane, P. F. Bedaque, K. Orginos and M. J. Savage, Phys. Rev. D **73**, 054503 (2006).
- [45] J. W. Chen, D. O'Connell, R. S. Van de Water and A. Walker-Loud, Phys. Rev. D **73**, 074510 (2006) [arXiv:hep-lat/0510024].
- [46] J. W. Chen, D. O'Connell and A. Walker-Loud, Phys. Rev. D **75**, 054501 (2007) [arXiv:hep-lat/0611003].
- [47] D. B. Renner *et al.*, Nucl. Phys. Proc. Suppl. **140**, 255 (2005).
- [48] R. G. Edwards *et al.*, PoS **LAT2005**, 056 (2005).
- [49] K. Orginos, D. Toussaint and R. L. Sugar, Phys. Rev. D **60**, 054503 (1999).
- [50] K. Orginos and D. Toussaint, Phys. Rev. D **59**, 014501 (1999).
- [51] C. W. Bernard *et al.*, Phys. Rev. D **64**, 054506 (2001).
- [52] A. Hasenfratz and F. Knechtli, Phys. Rev. D **64**, 034504 (2001).
- [53] T. A. DeGrand, A. Hasenfratz and T. G. Kovacs, Phys. Rev. D **67**, 054501 (2003).
- [54] T. A. DeGrand, Phys. Rev. D **69**, 014504 (2004).
- [55] S. Dürr, C. Hoelbling and U. Wenger, Phys. Rev. D **70**, 094502 (2004).
- [56] S. R. Beane, P. F. Bedaque, T. C. Luu, K. Orginos, E. Pallante, A. Parreño and M. J. Savage [NPLQCD Collaboration], arXiv:hep-lat/0612026.
- [57] S. R. Beane, P. F. Bedaque, T. C. Luu, K. Orginos, E. Pallante, A. Parreño and M. J. Savage, Phys. Rev. D **74**, 114503 (2006) [arXiv:hep-lat/0607036].
- [58] D. B. Kaplan, Phys. Lett. B **288**, 342 (1992) [arXiv:hep-lat/9206013].
- [59] Y. Shamir, Phys. Lett. B **305**, 357 (1993) [arXiv:hep-lat/9212010].
- [60] Y. Shamir, Nucl. Phys. B **406**, 90 (1993) [arXiv:hep-lat/9303005].
- [61] Y. Shamir, Phys. Rev. D **59**, 054506 (1999) [arXiv:hep-lat/9807012].
- [62] V. Furman and Y. Shamir, Nucl. Phys. B **439**, 54 (1995) [arXiv:hep-lat/9405004].
- [63] *Lattice Methods for Quantum Chromodynamics*, by Thomas DeGrand and Carleton DeTar, World Scientific, ISBN 981-256-727-5 (2006).
- [64] S. Dürr and C. Hoelbling, Phys. Rev. D **71**, 054501 (2005) [arXiv:hep-lat/0411022].
- [65] M. Creutz, arXiv:hep-lat/0603020.
- [66] C. Bernard, M. Golterman, Y. Shamir and S. R. Sharpe, arXiv:hep-lat/0603027.

- [67] S. Dürr and C. Hoelbling, arXiv:hep-lat/0604005.
- [68] A. Hasenfratz and R. Hoffmann, arXiv:hep-lat/0604010.
- [69] C. Bernard, M. Golterman and Y. Shamir, Phys. Rev. D **73**, 114511 (2006) [arXiv:hep-lat/0604017].
- [70] Y. Shamir, arXiv:hep-lat/0607007.
- [71] S. R. Sharpe, PoS **LAT2006**, 022 (2006) [arXiv:hep-lat/0610094].
- [72] J. W. Chen, D. O'Connell and A. Walker-Loud, arXiv:0706.0035 [hep-lat].
- [73] M. Lüscher, Commun. Math. Phys. **104**, 177 (1986).
- [74] J. Gasser and H. Leutwyler, Phys. Lett. B **188**, 477 (1987).
- [75] P. F. Bedaque, I. Sato and A. Walker-Loud, Phys. Rev. D **73**, 074501 (2006) [arXiv:hep-lat/0601033].
- [76] M. Golterman and Y. Shamir, Phys. Rev. D **71**, 034502 (2005) [arXiv:hep-lat/0411007].
- [77] J. Gasser and H. Leutwyler, Nucl. Phys. B **250**, 465 (1985).
- [78] A. Manohar and H. Georgi, Nucl. Phys. B **234**, 189 (1984).
- [79] R. G. Edwards and B. Joo [SciDAC Collaboration], [arXiv:hep-lat/0409003].